Pakistan J. Zool., pp 1-13, 2021. **DOI**: https://dx.doi.org/10.17582/journal.pjz/20191010081058

Dual Targeting of Janus Kinase and Bruton's Tyrosine Kinase: A New Approach to Control the Pathogenesis of Rheumatoid Arthritis

Neelam Pery[1]*, Fatima Ijaz[1], Nayab Batool Rizvi[1], Munawar Ali Munawar[1] and Muhammad Imtiaz Shafiq[2]*

[1]*Institute of Chemistry, University of the Punjab, Lahore, Pakistan 54590*
[2]*Institute of Biochemistry and Biotechnology, University of the Punjab, Lahore-54590*

ABSTRACT

Rheumatoid arthritis is an autoimmune disease with prevalence all over the world. Several therapeutics with different modes of action are available to deal with the disease but have failed to produce universal response leaving a large proportion of patients untreated. This is due to complex pathogenesis comprising a network of signaling pathways. By controlling one pathway, the pathogenesis continues through complementary pathways. Janus kinase and bruton's tyrosine kinase regulates a number of T-cell and B-cell mediated signaling pathways ranging from cytokine expression and antibody production to the bone resorption and cartilage destruction. We propose a dual trap to control this pathogenesis in the form of dual JAK3/BTK inhibitor. Using the computer-aided drug designing techniques, we developed dual JAK3 and BTK inhibitors based on quinoxaline derivatives which show appreciable dual inhibition in enzyme assays. To our knowledge, this is the first-ever report on dual JAK3/BTK inhibitors.

Article Information
Received 10 October 2019
Revised 02 December 2019
Accepted 12 December 2019
Available online 18 June 2020

Authors' Contribution
NP performed *in-silico* enzyme studies and drug designing under the supervision NBR and IS. FI did organic synthesis under the supervision of MAM.

Key words
Rheumatoid arthritis, Janus kinase, Bruton's tyrosine kinase, Molecular docking, Dual inhibition

INTRODUCTION

Rheumatoid arthritis (RA), an autoimmune disease has been a serious problem for clinicians for a long time. Biologic drugs such as TNFα inhibitors, IL-1 inhibitors, IL-6 inhibitors and co-stimulatory signal inhibitors entered the RA therapeutics with the advent of twenty-first century and have been very successful in improving the signs and symptoms of the disease reducing joint deformity and disability (Camean-Castillo *et al*., 2019; Smolen *et al*., 2017). TNFα inhibitors as monotherapy or in combination with methotrexate (conventional drug) have been quite successful in halting the disease and producing radiographic improvements (Boyce *et al*., 2010; Bruce and Boyce, 2007; Orme *et al*., 2012; Singh *et al*., 2009). However, unfortunately, this response is achieved only in 30% of the patients (Tanaka *et al*., 2013). Patients showing appreciable response rate need a long term medication as early termination of therapy results in reinstating of the symptoms almost in 50-80% of the patients (Tanaka *et al*., 2013). There is also an issue of the development of antibodies against the biologics causing it to be less efficacious (Kotyla, 2018). The lack of universal response, reduced efficacy on prolonged intake, unendurable adverse effects, subcutaneous or intravenous mode of administration along with high cost added up to the urge for new orally available, more efficacious and cheaper therapeutics for rheumatoid arthritis. This was further accompanied with the understanding of RA pathogenesis and identification of tyrosine kinases along with their roles in autoimmune diseases.

Tyrosine kinases control the cellular signal transduction pathways initiated by the cytokines. The auto-immune response stimulated by cytokines such as activation and differentiation of the cells, proliferation, release of inflammatory cytokines and chemokines and even the production of particular enzymes and antibodies is at the core systematized by the tyrosine kinases. These act as intracellular mediators which on receiving the signals through specific cytokines regulate the nuclear transcription and cellular response. By intervening with these kinases, the signal transduction pathways can be superseded and cellular response can be modified. Thus tyrosine kinases became new targets for rheumatoid arthritis and tremendous research started to look for novel orally available kinase inhibiting drugs (D'Aura Swanson *et al*., 2009). Important kinases involved in RA pathogenesis which have been targeted so far are p38 mitogen-activated protein kinase (p38MAPK), spleen-tyrosine kinase (SYK), janus kinase (JAK) and burton's tyrosine kinase (BTK) (D'Aura Swanson *et al*., 2009). Efforts to target p38 mitogen-activated protein kinase (p38MAPK) and spleen-tyrosine kinase (SYK) have not

* Corresponding author: neelam.wafa@gmail.com; imtiaz.ibb@pu.edu.pk
0030-9923/2021/0004-0001 $ 9.00/0

been very fruitful in terms of superiority to methotrexate and issues with safety profile (Meier and McInnes, 2014). However, JAK and BTK seem promising to fulfill higher hopes associated with kinase inhibiting drugs in oncology and anti-inflammatory diseases. The JAK inhibitors have shown higher efficacy and superiority to methotrexate (MTX) as monotherapy or in combination with MTX (Onuora, 2014; Taylor, 2019). JAK kinases have four members JAK1, JAK2, JAK3, and TYK2, all activated by the interaction of cytokines with their receptors on the cell surface. On activation, these activate signal transducers and activators of transcription (STAT) proteins which then dimerize and pass to the nucleus where these regulate the expression or silencing of the genes. The pathways thus controlled are called as JAK-STAT pathways. JAK-STAT signaling has been found to regulate the complex interplay between cellular metabolism and inflammation in rheumatoid arthritis (Schwartz *et al*., 2017). The JAK-STAT pathways are involved in signaling through many cytokines and IFNα, IFNβ, IL-6, IL-7, IL- 10, IL-12, IL-15, IL-21 and IL-23. It is also involved in signaling pathways leading to the production of metalloproteinase-9 (MMP-9), an important mediator of cartilage destruction (Atzeni *et al*., 2018).

Out of the four forms, JAK3 is particularly crucial for the expression of IL-2, 4, 7, 9, 15 and 21. It is involved in lymphocyte development and survival. JAK3 expression is limited to myeloid and lymphoid cells and hence it seems to be the most attractive target for anti-inflammatory drugs. It is involved in lymphocyte development and survival (Roskoski, 2016). Development of SCID (severe combined immunodeficiency) due to loss of function of JAK3 encoding genes emphasized its role in immune response (Russell *et al*., 1994; 1995). Deficiency of JAK3 also has been found to block innate lymphoid cells (ILC) differentiation in bone marrow. All this highlights its role in anti-inflammatory diseases. Higher-level expression of JAKs and STATs in the RA synovium further augments their importance as a therapeutic target to control rheumatoid arthritis (Walker *et al*., 2006a, b). Tofacitinib is the first JAK inhibitor approved by the FDA in 2012 for the treatment of rheumatoid arthritis in cases of inadequate response to methotrexate. Tofacitinib has shown enhanced efficacy as monotherapy and in combination with methotrexate (Clark *et al*., 2014; Fleischmann *et al*., 2012). Since then extensive research is going on to explore more efficacious JAK inhibitors with lesser safety issues. Baricitinib is the second FDA approved JAK inhibitor but it inhibits JAK1/2 more than JAK3 and TYK2. It has been approved for adult patients with moderate to severe disease activity and previous failure to TNFα inhibiting therapies (Markham, 2017). A boxed warning is issued with Baricitinib for the increased risk of malignancies, thrombosis and serious infections (Atzeni *et al*., 2018). It is in clinical trials to evaluate the safety of its long term use. An extensive research is going on to explore more efficacious JAK inhibitors with lesser safety issues.

Bruton's tyrosine kinase, a member of cytoplasmic non-receptor Tec family kinases, is expressed in macrophages, neutrophils, mast cells, and B-cells. It is involved in signaling through B cell receptor (BCR) and Fcγ receptor (FcR) controlling the activation, survival, differentiation, and proliferation of B-cells (Haselmayer *et al*., 2019). By controlling the BCR signaling, BCR dependent proliferation can be regulated leading to controlled expression of co-stimulatory molecules and pro-inflammatory cytokines. BTK also regulates the signal transduction pathways of activated IgG immune complexes in the synovial fluid of RA patients and stimulates the production of inflammatory cytokines, chemokines and matrix metalloproteinases from synovial macrophages (Park *et al*., 2016). Higher levels of BTK make the innate cells to infiltrate the synovial cavity and to produce inflammatory cytokines. Through receptor activator of nuclear factor kappa-B (RANK), BTK regulates the bone resorption. It stimulates osteoclast activation and differentiation leading to bone destruction (Bajpai *et al*., 2000). Blocking BTK has been proved to be an efficient strategy to control RA and B-cell dependent malignancies (Di Paolo *et al*., 2011). BTK inhibitor Ibrutinib has been approved by the FDA for B-cell malignancies (Cameron and Sanford, 2014) but there is currently no approved BTK therapy for rheumatoid arthritis.

In spite of the availability of therapeutics with different modes of action, a large proportion of patients remain unresponsive showing an unmet need for therapies with enhanced efficacy and universal response rate. This may be attributed to the involvement of multiple pathways in the pathogenesis of the disease. When we attack one pathway the pathogenesis continues through other interlinking pathways. We propose a dual JAK and BTK inhibitor to control rheumatoid arthritis; a multigenic trap for a multigenic disease. The concept of dual inhibition; a multi-target directed therapy has been developed in the last two decades to deal with the diseases involving complex pathogenesis. Dual 5-LOX/COX inhibitors for anti-inflammatory drugs (Martel-Pelletier *et al*., 2003), dual AChE/MAO inhibitors for Alzheimer's disease (Sterling *et al*., 2002) and dual MDM2/MDMX inhibitors to fight with cancer (Chang *et al*., 2013) are few examples. Dual JAK3/BTK inhibition seems promising to deal with rheumatoid arthritis. The JAK3 inhibition will control the STAT pathways regulating inflammatory cytokines while BTK inhibition will attack the disease on another front by

controlling BTK mediated signaling pathways. Here we report the identification of quinoxaline derivatives as dual JAK3/BTK inhibitors.

Quinoxaline derivatives have attracted great attention in pharmaceutical industry due to a variety of biological activities associated with them such as antimicrobial, anti-depressant, anti-proliferative, anti-inflammatory and anti-cancer activities (Pereira *et al*., 2015; Tariq *et al*., 2018b). Quinoxaline derivatives have been explored as protein tyrosine kinase inhibitors (El Newahie *et al*., 2016; Patinote *et al*., 2017). Studies have shown these derivatives as potent inhibitors of p38α MAP kinase, human protein kinase CK2, EFGR tyrosine kinase and phosphoinositide 3-kinase (PI3K) inhibitors (Guillon *et al*., 2013; Qin *et al*., 2015; Tariq *et al*., 2018a; Wu *et al*., 2012). Some chalcone derivatives containing Triazolo [4,3-a]-quinoxaline moieties have been reported as dual EFGR kinase and tubulin polymerization inhibitors to control cancer (Alswah *et al*., 2017). The quinoxaline nucleus in the main precursor in these derivatives that is responsible for the diverse biological activities (Pereira *et al*., 2015). It shows the potential of quinoxaline derivatives to be designed and modified to get diverse and desirable biological activities.

We have designed a number of quinoxaline derivatives and predicted their binding mode using molecular docking tools. The compounds showing a promising binding mode in both the enzymes (JAK3 and BTK) were put to synthesis and biological evaluation. To our knowledge, it is the first-ever report on dual JAK3/BTK inhibitors and opens new avenues to search for more efficacious therapies for oncology and anti-inflammatory diseases.

MATERIALS AND METHODS

Structure retrieval from the database

The work was started by comparing the binding sites of the janus kinase 3 (JAK3) and bruton's tyrosine kinase (BTK). Structure of JAK3 (PDB ID: 5LWM) and BTK (PD ID: 5P9K) were downloaded from the protein data bank. A BLAST search was run to get a list of all available PDB structures. BLAST uses a special format called as FASTA format. The FASTA sequences of JAK3 (PDB ID: 5LWM) and BTK (PDB ID: 5P9K) obtained from the protein data bank were used as input for protein-protein BLAST using non-redundant protein sequences(nr) database for homosapiens. From the BLAST output, the PDB structures with a resolution of 2.5 Å or less and having an enzyme in complex with the inhibitors, representing the active form of enzymes were analyzed for investigating the vowing features of binding pocket.

Analysis of the binding cavities

PyMOL molecular viewer 2.0.1 was used to investigate hydrogen bonding interactions within 2.4 to 4 Å of protein-ligand contact while the hydrophobic interactions were explored with Discovery Studio client 2016 (BIOVIA, 2016; DeLano, 2002). The structural alignment of the two proteins was done with PyMOL while pairwise alignment tool EMBOSS Matcher was used to align the protein sequences (Rice *et al*., 2000). The information obtained from these results was used to analyze the regions of the binding cavity of both enzymes offering similar or different interactions and thus infer the possibility of developing dual inhibitors.

Drug designing and molecular docking

The quinoxaline derivatives were selected to have hydrogen bond donor and acceptor centers at positions suitable to interact with the ATP binding residues of the two enzymes. Some other substituents were added to offer some hydrophobic interactions and a sustained fit in the binding cavity. Bigger substituents were avoided to rule out any chances of steric clashes in two different binding pockets. The designed compounds were docked against JAK3 and BTK using Autodock vina and binding pose was analyzed. Derivatives having a suitable binding pose in both the enzymes were put to synthesis.

Receptor and ligand preparation for molecular docking

Ligands were removed from the PDB files and protein structures were prepared by removing water molecules and adding gasteiger charges and polar hydrogens using Autodock tools (ADT) 4.2 (Morris *et al*., 2009). Ligand structures were drawn and 3D optimized with ChemSketch (ACD/ChemSketch (freeware), 2012). Avogadro software was used for energy minimization applying the Ghemical force field and steepest descent algorithm with four steps per update (Hanwell *et al*., 2012). Ligands were prepared for docking with ADT tools by adding gasteiger charges and selecting torsion and saved as PDBQT files. Docking was run using Auto Dock Vina (Trott and Olson, 2010). The docking protocols were validated by running test experiment of docking tofacitinib and other reported inhibitors (Boggon *et al*., 2005; Chrencik *et al*., 2010; de Vicente *et al*., 2014; Farmer *et al*., 2015; Goedken *et al*., 2015; Hennessy *et al*., 2016; Jaime-Figueroa *et al*., 2013; Lynch *et al*., 2013; Soth *et al*., 2013; Thoma *et al*., 2011). The interactions and poses obtained by docking results were compared with the reported crystal structure interactions which proved higher identity within accepted rmsd range (rmsd< 2 Å). The success rate was found to be 80 %.

Synthesis of selected inhibitors

All the chemicals including solvents and reagents were obtained from commercial sources such as Acros, Alfa Acer and Sigma Aldrich. Commercial ethanol was dried using calcium oxide and then distilled to get absolute ethanol. Thin layer and column chromatography were performed with "Merck silica gel 60F plate". Melting points were determined with a "Gallenkamp melting point apparatus". IR spectra were recorded using "Agilent Cary Technologies 630 FT-IR with diamond ATR" within the spectral range of 4,000 and 400 cm-^{1} whereas ^{1}H-NMR spectra were taken in chloroform-*d*, methanol-*d*, acetone-*d* or DMSO-*d* on "Bruker Avance NMR instrument". Enzyme inhibition studies were performed using enzyme-linked immunosorbent assay (ELISA) and IC50 values were computed using EZ-FitTM Enzyme Kinetics Software.

RESULTS AND DISCUSSION

Comparison of the JAK3 and BTK binding sites

Both the enzymes have typical bi-lobed structure of protein tyrosine kinases. The sequence alignment results show these proteins to have a similar primary structure with 32.7% identity (67/205), 58.5% similarity (120/205) and 4.9% (10/205) gaps with a score of 266 (sequence alignment is given in Supplementary material). The two proteins have higher folding and conformational similarity. Although at some places the length and the positioning of the loops is slightly different, overall folding mode, the positioning of the lobes, the helical structure and β plates, as well as the binding groove at hinge region, show many similarities (Fig. 1). The RMSD of the two aligned structures comes out to be 5.056 Å. In BTK, the structure is more compact and closed while in JAK3 it seems to be in slightly expanded form. The C-terminal lobes of both enzymes show many similarities in their orientation. However, from the hinge loop upwards, the BTK is slightly bent towards the right side making it compact. Although, the glycine loop in JAK3 is hanging lower than that in BTK but its activation loop after the DFG motif bends downwards and is low lying. This gap between the glycine loop and the activation loop makes the binding grove relatively open at the end. While in BTK, the activation loop is raised up and lies close to the glycine loop which closes the end of the binding groove at the tip. It makes the binding groove of the BTK to lie deep inside and close at the end.

Binding pockets of JAK3 and BTK were overlaid to investigate the similarities and differences in their active site residues and to explore regions having the same or equivalent environment (Fig. 2). This analysis has revealed the potential role of different residues of both the enzymes towards the designing of dual inhibitors. Surprisingly, in both the enzymes, same or equivalent residues occupy similar positions. ALA 853 of JAK3 hangs over the binding groove from the N-terminal lobe; BTK has ALA 428 at the same position. Similarly, LEU 956 lies at the floor of the front pocket of the JAK3 binding cavity. BTK also has LEU 528 at equivalent position although the orientation of both the residues is slightly different from each other; both have been seen highly efficient in developing hydrophobic interactions with inhibitors. LEU 828 of the glycine loop in JAK3 has the same orientation as LEU 408 from the glycine loop of BTK and both have shown a higher rate of interactions with the inhibitors in reported structures. CYS 909 of JAK3 is at the same position and orientation in JAK3 as the CYS 481 of BTK and in both the enzymes this cysteine is involved in forming covalent interactions with the covalent inhibitors (Awan and Jurczak, 2018; Evans *et al*., 2013; Goedken *et al*., 2015; Kempson *et al*., 2017; Wu *et al*., 2017). One of the hinge ATP binding residues, GLU 903 in JAK3 and GLU 575 in BTK, is also the same in both the enzymes with similar orientation in the binding cavity.

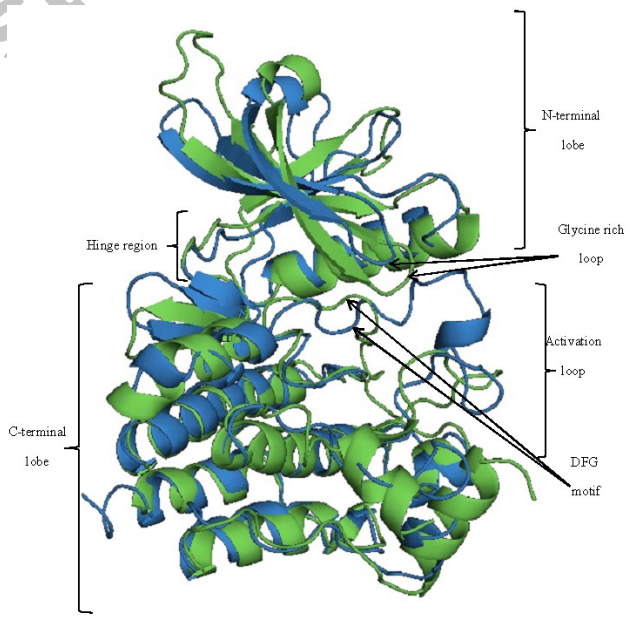

Fig. 1. Structural alignment of JAK3 (green) and BTK (blue). Both the structures are aligned with a RMSD of 5.056 Å.

The differing residues are present at three different points in the binding groove of the enzymes that may be responsible for rendering different binding affinities of these enzymes towards inhibitors. The first point of differentiation is the ATP binding hinge residue LEU 905 of

JAK3 and MET 475 of BTK. Leucine, just like methionine is a non-polar, aliphatic amino acid with an isobutyl side chain. Their interactive properties do not much differ. In both the enzymes, these residues are preceded by glutamine and tyrosine (GLU 903 and TYR 904 in JAK3 while GLU 475 and TYR 476 in BTK). These are the site for ATP binding and are most important to target by the inhibitors. These are at the same distance and angle with the GLU residue and offer similar interaction. In JAK3, the gatekeeper residue is MET 902 having a longer side chain as compared to that of THR 474 of BTK. This longer side chain blocks the upper backside of the binding cavity making it relatively less deep. Alanine (ALA 966) with a methyl side chain lies at the floor of the binding pocket in JAK3. BTK has SER 538 at a relevant position. It makes the lower floor of the binding groove of BTK a bit hydrophilic; however, its hydroxymethyl side chain is directed away from the binding groove reducing this effect. Other than these differences, most of the residues contribute similar interaction behavior towards inhibitors. This along with similar shape of the binding cavities encouraged the development of dual JAK3 and BTK inhibitors.

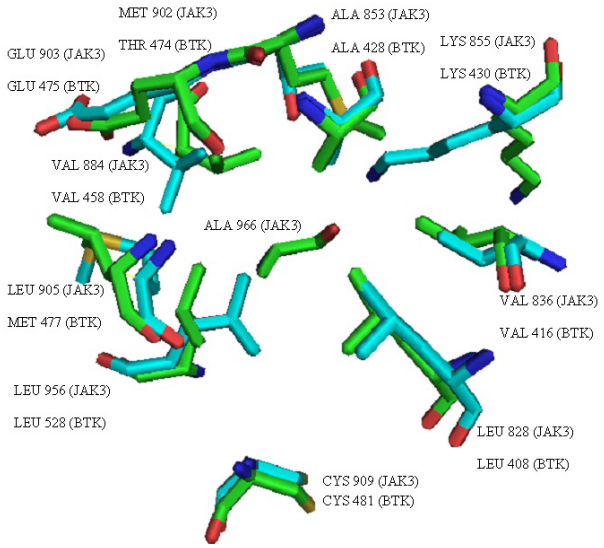

Fig. 2. Overlay of active sites of JAK3 (green) and BTK (blue) representing the residues found interacting in the reported enzyme-inhibitor complexes.

Molecular docking of designed inhibitors and predicting their binding pose

Quinoxaline itself was docked against JAK3 and BTK. Although its ring nitrogen develops a hydrogen bond to the LEU 905 and MET 477 but in most of the conformations, this hydrogen bonding interaction is lost. This can be attributed to its very small size and lack of polar centers in the moecule to develop polar interactions with various residues lining the binding cavity. To overcome this problem, nitro and amino quinoxalines were selected to be explored as dual inhibitors. The nitro group introduces hydrogen bond acceptors to the ligand molecule and amino group introduces hydrogen bond donor centers.

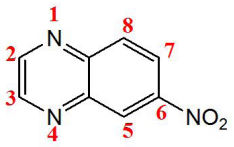

6-nitroquinoxaline

(1)

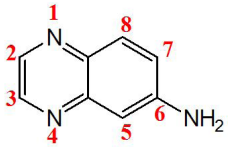

quinoxalin-6-amine

(2)

The ATP binding site residues of JAK3 comprises of GLU 903 and LEU 905 while those of BTK comprise of GLU 475 and MET 477. The orientation of GLU residue in the binding pocket is such that it acts a hydrogen bond acceptor in ligand binding. While LEU and MET both have their NH towards the binding cavity and act as hydrogen bond donors. So, the 6-nitroquinoxaline having only the hydrogen bond acceptor region bind only to the LEU 905 (JAK3) or MET 477 (BTK) residues of the bindig cavity. The amino group in quinoxalin-6-amine, introduces hydrogen bond donors to the quinoxaline molecule that previously contained only hydrogen bond acceptors. This ligand now can acts as hydrogen bond donor and interacts with GLU residue of the binding cavity through its amine group or as hydrogen bond acceptor through its ring nitrogen.

This is seen by analysing the docking results of both the compounds in the binding pockets of JAK3 and BTK (Fig. 3). Niroquinoxaline makes a hydrogen bond with the LEU 905 of JAK3 and MET 477 of BTK. However in BTK, it also hydrogen bonds with the 'NH' of the side chain of LYS 430. The eqivalent LYS 855 residue in JAK3 is having its side chain oriented away from the hinge region and no such interaction is seen. On the other hand, quinoxalin-6-amine in both the enzymes is developing hydrogen bond to the glutamic acid (GLU) residues. Although the interaction between ring nitrogen of quinoxaline moiety and hydrogen bond donor leucine residue, is also seen in some docked coformations of JAK3 but the lowest energy conformation shows the bonding with glutamic acid residue. It was expected that amino derivative will show better binding affinity but the reverse is observed through Autodock vina produced binding affinity values (Table I).

Different alkyl groups were substituted at positions 2, 3 and 7 of the two compounds. The substituents were designed in such a way to explore the effects of smaller

to bigger alkyl groups on the hydrophobic interactions of the ligand in the binding cavity. In this way 20 different ligands were designed and docked against JAK3 and BTK. The substitutuion at position 7 was not fruitful as it resulted in the loss of hydrogen bonding interactions between the ligand molecule and the ATP binding residues of the binding cavity. Out of all the designed ligands, eight (Fig. 4) were able to produce favourable binding pose and appreciable binding affinity value in both the enzyme molecules.

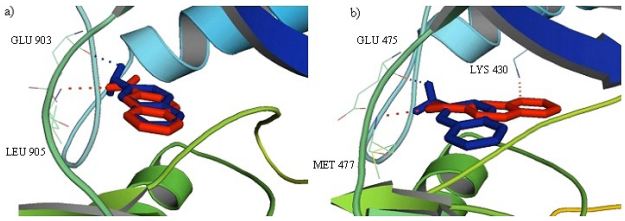

Fig. 3. Cartoon representation of the JAK3 (a) and BTK (b) with an overlay of 6-nitroquinoxaline (Red) and quinoxalin-6-amine (Blue) in the binding cavity highlighting the hydrogen bonding residues. Dotted lines show hydrogen bonding.

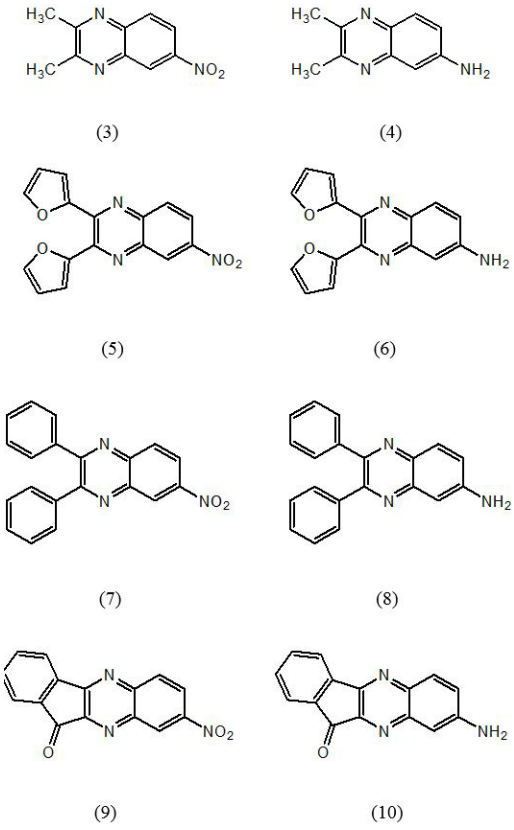

Fig. 4. Structures of quinoxaline derivatives showing appreciable binding mode in both the enzymes (JAK3 and BTK).

In JAK3, dimethyl and diphenyl nitro derivatives (3 and 7) just like the 6-nitroquinoxaline molecule, hydrogen bond with the LEU 905 of the hinge ATP binding region. A better value of binding affinity is seen with diphenyl derivative that can be attributed to the hydrophobic interactions of the diphenyl rings with the rsidues from the upper and lower lobe. Ligand 5 show an additional hydrogen bond with the CYS 909 residue from the extended hinge region and its binding affinity value is slightly better than that for diphenyl derivative. Ligand 9 show much stronger bonding with the hinge residues through three hydrogen bonds which is depicted in its higher binding affinity values. Amino derivatives have comparable binding pose and binding affinity to that of nitro derivatives. The amino derivatives develop a hydrogen bond to the GLU 903 instead of LEU 905 seen in case of nitro derivatives. Ligand 10 is an exception to this as it makes a hydrogen bond to the LEU 905 and PRO 906. In amino derivatives, the interaction with GLU 903, brings the ligand molecule in a position to have some hydrophoic intearctions with the ALA 853 from the upper lobe. The hydophobic interactions with the VAL 836, ALA 853, VAL 884 and ALA 966 are seen in all the ligand complexes. The quinoxaline ring is in pi-sigma hydrophobic interactions with the LEU 956 from the lower lobe and LEU 828 from the upper lobe in all the nitro and amino derivatives (Fig. 5a and 5b). In difuran derivative, the furan rings are in pi-anionic interactions with ASP 912 from the lower lobe.

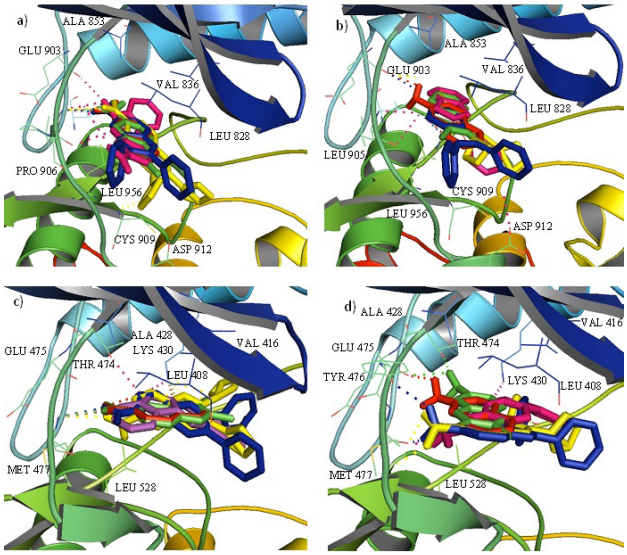

Fig. 5. Cartoon representation of the JAK3 (upper) with an overlay of 6-nitroquinoxaline derivatives (a) and quinoxalin-6-amine derivatives (b) and BTK (lower) with an overlay of 6-nitroquinoxaline derivatives (c) and quinoxalin-6-amine derivatives (d) in the binding cavity highlighting the interacting residues. Dotted lines show hydrogen bonding.

In BTK, all the nitro derivatives retain the two hydrogen bonds with MET 477 and LYS 430 seen in the parent compound 6-nitroquinoxaline. In ligand 8, the appreciable value of binding affinity is observed although the hydrogen bond with the LYS 430 is lost. It may be attributed to the hydrophobic interactions between the phenyl moiety and residues from the upper and lower lobes. The phenyl ring develops pi-anionic interactions with the ASP 539 from the lower lobe. Ligand 9 is in hydrogen bond with the THR 474, the gate keeper residue and LYS 430 showing the highest value of binding affinity. The nitro derivatives show higher binding affinity for BTK as compared to JAK3. The quinoxaline ring is in pi-sigma interactions with VAL 416 and pi-alkyl interactions with the LEU 528 from the lower lobe and LEU 408 and ALA 428 from the upper lobe in all the complexes formed.The quinoxaline-6-amine show reduced value of bindig affinity as compared to the 6-nitroquinoxaline. Its interactions with the GLU 475, brings its amino 'NH' in close proxmity of MET 477 craeting donor-donor clashes. This problem is not seen in 4, where the amino group interacts with THR 474 and GLU 475. The other derivatives show a hydrogen bond between the amino group and the MET 477 residue. However, these show higher value of binding affinity than the dimethyl derivative (4) which can be attributed to the hydrophobic interactios between their larger alkyl groups and the residues from the upper and lower lobes. The quinoxaline ring develops pi-sigma hydrophobic interactions with VAL 416 and pi-alkyl hydrophobic interactions with the LEU 528 from the lower lobe and LEU 408 and ALA 428 from the upper lobe in all the ligand complexes formed. No stearic clashes between the ligands and both the enzymes are seen and these are able adapt the shape complimentarity of the binding cavities (Fig. 6).

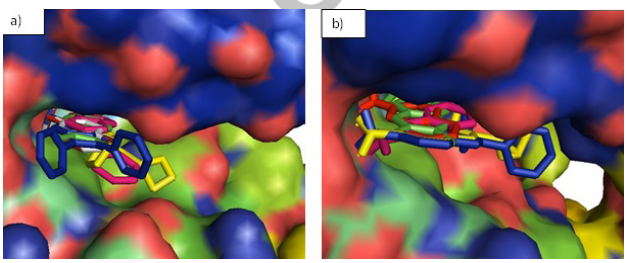

Fig. 6. Surface representation of the designed inhibitors in the binding pocket of JAK3 (a) and BTK (b). The inhibitors fit well in the binding groove of both the enzymes and no clashes are seen.

Synthesis of selected dual inhibitors

After analysis of the docking results, the designed inhibitors were put to synthesis. Nitro derivatives were prepared by the condensation reaction of 4-nitro-*o*-phenylenediamine and vicinal diketones in refluxing ethanol/acetic acid mixture (1:1). The nitro derivatives were then converted to respective amino derivatives using catalytic reduction with hydrazine hydrate in the presence of palladium charcoal.

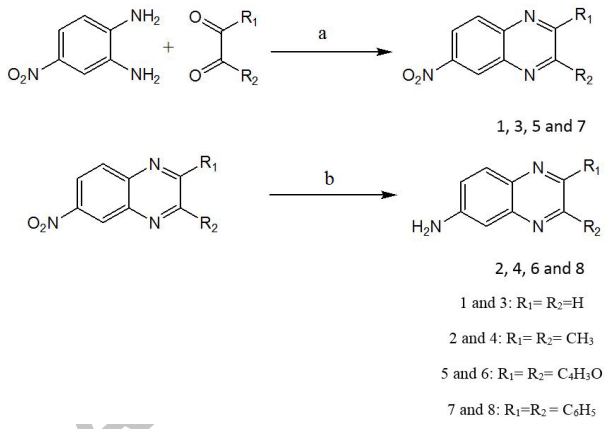

Fig. 7. Synthetic scheme I: Reagents and conditions: (a) AcOH/ EtOH, Reflux 2-3 h, -H_2O (b) $NH_2NH_2.H_2O$, Pd/C, EtOH, reflux 2h.

For compounds 9 and 10, ninhydrin was used with 4-nitro-*o*-phenylenediamine in equimolar quantities in refluxing ethanol/acetic acid mixture. However, a mixture of non-separable 9a and 9b was formed. The reduction of this mixture gave 10a and 10b.

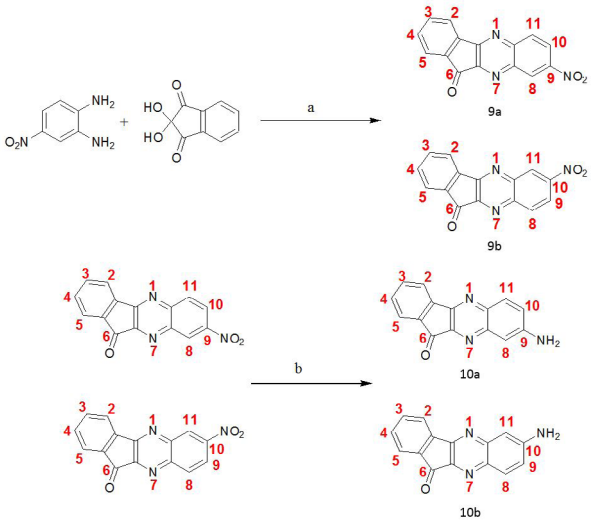

Fig. 8. Synthetic scheme II. Reagents and conditions: (a) AcOH/ EtOH, Reflux 2-3 hrs, -H_2O (b) $NH_2NH_2.H_2O$, Pd/C, EtOH, reflux 2.

Table I. Binding affinity values (predicted by molecular docking) and the IC 50 (from enzyme inhibition studies) value for JAK3 and BTK.

Serial number	Ligand ID	Binding affinity Δ G (kcal/mol) for JAK3	IC 50(μM) values for JAK3	Binding affinity Δ G (kcal/mol) for BTK	IC 50(μM) values for BTK
1	1	-5.7	132.24	-6.1	47.63
2	2	-5.7	97.42	-5.7	392.54
3	3	-6.2	87.51	-6.7	59.32
4	4	-6.4	80.07	-6.3	73.17
5	5	-7.1	58.37	-8.4	5.82
6	6	-7.2	92.31	-7.7	26.72
7	7	-6.9	74.09	-8.2	8.41
8	8	-6.8	76.20	-7.4	91.06
9	9	-8.1(-8.8*)	5.47	-8.9(-8.3*)	13.58
10	10	-8.8(-7.7**)	6.78	-7.9(-8.1**)	13.94

* Binding affinity for 5b compound; **Binding affinity for 10b compound.

Figure 7 shows synthetic scheme I and Figure 8 show s synthetic scheme II. The experimental data of the synthesized compounds is given in supplementary material.

Docking score and enzyme inhibition

The compounds with appropriate binding pose and reasonable values of binding affinity as predicted by the docking program were preceded to enzyme inhibition studies. The IC50 value for JAK3 and BTK are given in Table I.

In the ideal situation, the compounds with a more negative binding affinity (predicted by molecular docking program) should have a lower IC50 value in enzyme inhibition assays. This is in accordance with our results from enzyme inhibition studies with some minor variations. In BTK, the ligand 2 is having a higher value of IC50 as compared to the ligands having comparable binding affinity value. This can be due to the unfavorable donor-donor clashes seen in the molecular docking. Similarly, in JAK3, the ligand 6 is showing a higher IC50 value as compared to the ligand 4 and 8 although its having better predicted binding affinity than these. But as the difference is small so can be ignored. Ligand 9 and 10 show some differences in the IC50 value as compared to what was expected based on binding affinity values given by docking program. It may be due to the fact that it is a mixture of compound 9a and 9b and 10a and 10b. The docking score of 9b does not show as good binding as that for 9a. Interaction of the inhibitor with ATP binding hinge residues is not seen for 9b. In case of ligand 10, both the 10a and 10b are having almost equal binding affinity value so this effect is not so prominent. The ligand 9, the nitro derivative and its respective amino derivative 10 show better results for JAK3 as compared to BTK. An unexpectedly higher IC50 value is achieved for inhibitor 1 in JAK3 and inhibitor 8 in BTK. These results are consistent with the 80% success rate of the docking protocol determined in the validation process. IC50 values in micro molar quantities achieved in enzyme inhibition assays validate the docking protocol and use of computer-aided drug designing approaches to search for new therapeutics. Computer aided drug designing techniques reduce the time and cost for the identification of new drugs. The appreciable enzyme inhibition achieved confirms the probability of developing dual JAK3 and BTK inhibitors.

CONCLUSION

Rheumatoid arthritis is an autoimmune disease involving complex pathogenesis. The medications available with different modes of action to attack the disease at different fronts fail to produce a universal response and a large proportion of patients remain unresponsive. By the blockage of one pathway, the pathogenesis continues through complementary pathways. We proposed a multigenic trap in the form of dual JAK3 and BTK inhibitors. The binding pockets of both the enzymes were compared to assess the possibility of developing dual inhibitors and then *in silico* drug designing techniques were used to identify molecules able to interact with both the enzymes. Nitro and amino-quinoxaline derivatives have been proved to be promising dual JAK3/BTK inhibitors. These can be optimized to further enhance their efficacy

and selectivity. These results open avenues for the search of more efficacious drugs producing universal response rate. Dual JAK3 and BTK inhibitors can fulfill the unmet need of therapeutics able to control disease pathogenesis in larger proportion of the patients. To our knowledge, it is the first-ever report on dual JAK3/BTK inhibitors.

Supplementary material

There is supplementary material associated with this article. Access the material online at: https://dx.doi.org/10.17582/journal.pjz/20191010081058

Statement of conflict of interest

The authors have declared no conflict of interest regarding the publication of this article.

REFERENCES

ACD/ChemSketch (freeware). 2012. Retrieved from http://www.acdlabs.com/resources/freeware/chemsketch/

Alswah, M., Bayoumi, A.H., Elgamal, K., Elmorsy, A., Ihmaid, S. and Ahmed, H.E.A., 2017. Design, synthesis and cytotoxic evaluation of novel chalcone derivatives bearing triazolo[4,3-a]-quinoxaline moieties as potent anticancer agents with dual EGFR kinase and tubulin polymerization inhibitory effects. *Molecules,* **23**: 48. https://doi.org/10.3390/molecules23010048

Atzeni, F., Talotta, R., Nucera, V., Marino, F., Gerratana, E., Sangari, D., Masala, I.F. and Sarzi-Puttini, P., 2018. Adverse events, clinical considerations and management recommendations in rheumatoid arthritis patients treated with JAK inhibitors. *Expert Rev. Clin. Immunol.,* **14**: 945-956. https://doi.org/10.1080/1744666X.2018.1504678

Awan, F.T. and Jurczak, W., 2018. Use of acalabrutinib in patients with mantle cell lymphoma. *Expert Rev. Hematol.,* **11**: 495-502. https://doi.org/10.1080/17474086.2018.1473030

Bajpai, U.D., Zhang, K., Teutsch, M., Sen, R. and Wortis, H.H., 2000. Bruton's tyrosine kinase links the B cell receptor to nuclear factor kappaB activation. *J. exp. Med.,* **191**: 1735-1744. https://doi.org/10.1084/jem.191.10.1735

Biovia, D.S., 2016. Discovery Studio Client. Dassault Systèmes, San Diego.

Boggon, T.J., Li, Y., Manley, P.W. and Eck, M.J., 2005. Crystal structure of the Jak3 kinase domain in complex with a staurosporine analog. *Blood,* **106**: 996-1002. https://doi.org/10.1182/blood-2005-02-0707

Boyce, E.G., Halilovic, J. and Stan-Ugbene, O., 2010. Golimumab: Review of the efficacy and tolerability of a recently approved tumor necrosis factor-alpha inhibitor. *Clin. Ther.,* **32**: 1681-1703. https://doi.org/10.1016/j.clinthera.2010.09.003

Bruce, S.P. and Boyce, E.G., 2007. Update on abatacept: a selective costimulation modulator for rheumatoid arthritis. *Annls Pharmacother.,* **41**: 1153-1162. https://doi.org/10.1345/aph.1K057

Camean-Castillo, M., Gimeno-Ballester, V., Rios-Sanchez, E., Fenix-Caballero, S., Vazquez-Real, M. and Alegre-Del Rey, E., 2019. Network meta-analysis of tofacitinib versus biologic treatments in moderate-to-severe rheumatoid arthritis patients. *J. clin. Pharm. Ther.,* **44**: 384-396. https://doi.org/10.1111/jcpt.12795

Cameron, F. and Sanford, M., 2014. Ibrutinib: first global approval. *Drugs,* **74**: 263-271. https://doi.org/10.1007/s40265-014-0178-8

Chang, Y.S., Graves, B., Guerlavais, V., Tovar, C., Packman, K., To, K.H., Olson, K.A., Kesavan, K., Gangurde, P., Mukherjee, A., Baker, T., Darlak, K., Elkin, C., Filipovic, Z., Qureshi, F.Z., Cai, H., Berry, P., Feyfant, E., Shi, X.E., Horstick, J., Annis, D.A., Manning, A.M., Fotouhi, N., Nash, H., Vassilev, L.T. and Sawyer, T.K., 2013. Stapled alpha-helical peptide drug development: a potent dual inhibitor of MDM2 and MDMX for p53-dependent cancer therapy. *Proc. natl. Acad. Sci. USA,* **110**: E3445-3454. https://doi.org/10.1073/pnas.1303002110

Chrencik, J.E., Patny, A., Leung, I.K., Korniski, B., Emmons, T.L., Hall, T., Weinberg, R.A., Gormley, J.A., Williams, J.M., Day, J.E., Hirsch, J.L., Kiefer, J.R., Leone, J.W., Fischer, H.D., Sommers, C.D., Huang, H.C., Jacobsen, E.J., Tenbrink, R.E., Tomasselli, A.G. and Benson, T.E., 2010. Structural and thermodynamic characterization of the TYK2 and JAK3 kinase domains in complex with CP-690550 and CMP-6. *J. mol. Biol.,* **400**: 413-433. https://doi.org/10.1016/j.jmb.2010.05.020

Clark, J.D., Flanagan, M.E. and Telliez, J.B., 2014. Discovery and development of Janus kinase (JAK) inhibitors for inflammatory diseases. *J. med. Chem.,* **57**: 5023-5038. https://doi.org/10.1021/jm401490p

D'Aura Swanson, C., Paniagua, R.T., Lindstrom, T.M. and Robinson, W.H., 2009. Tyrosine kinases as targets for the treatment of rheumatoid arthritis. *Nat. Rev. Rheumatol.,* **5**: 317-324. https://doi.org/10.1038/nrrheum.2009.82

de Vicente, J., Lemoine, R., Bartlett, M., Hermann, J.C., Hekmat-Nejad, M., Henningsen, R., Jin, S., Kuglstatter, A., Li, H., Lovey, A.J., Menke, J., Niu, L., Patel, V., Petersen, A., Setti, L., Shao,

A., Tivitmahaisoon, P., Vu, M.D. and Soth, M., 2014. Scaffold hopping towards potent and selective JAK3 inhibitors: discovery of novel C-5 substituted pyrrolopyrazines. *Bioorg. med. Chem. Lett.,* **24**: 4969-4975. https://doi.org/10.1016/j.bmcl.2014.09.031

DeLano, W.L., 2002. *The PyMOL molecular graphics system*. Delano Scientific, San Carlos.

Di Paolo, J.A., Huang, T., Balazs, M., Barbosa, J., Barck, K.H., Bravo, B.J., Carano, R.A., Darrow, J., Davies, D.R., DeForge, L.E., Diehl, L., Ferrando, R., Gallion, S.L., Giannetti, A.M., Gribling, P., Hurez, V., Hymowitz, S.G., Jones, R., Kropf, J.E., Lee, W.P., Maciejewski, P.M., Mitchell, S.A., Rong, H., Staker, B.L., Whitney, J.A., Yeh, S., Young, W.B., Yu, C., Zhang, J., Reif, K. and Currie, K.S., 2011. Specific Btk inhibition suppresses B cell- and myeloid cell-mediated arthritis. *Nat. chem. Biol.,* **7**: 41-50. https://doi.org/10.1038/nchembio.481

El Newahie, A.M., Ismail, N.S., Abou El Ella, D.A. and Abouzid, K.A., 2016. Quinoxaline-based scaffolds targeting tyrosine kinases and their potential anticancer activity. *Arch. Pharm. (Weinheim),* **349**: 309-326. https://doi.org/10.1002/ardp.201500468

Evans, E.K., Tester, R., Aslanian, S., Karp, R., Sheets, M., Labenski, M.T., Witowski, S.R., Lounsbury, H., Chaturvedi, P., Mazdiyasni, H., Zhu, Z., Nacht, M., Freed, M.I., Petter, R.C., Dubrovskiy, A., Singh, J., and Westlin, W.F., 2013. Inhibition of Btk with CC-292 provides early pharmacodynamic assessment of activity in mice and humans. *J. Pharmacol. exp. Ther.,* **346**: 219-228. https://doi.org/10.1124/jpet.113.203489

Farmer, L.J., Ledeboer, M.W., Hoock, T., Arnost, M.J., Bethiel, R.S., Bennani, Y.L., Black, J.J., Brummel, C.L., Chakilam, A., Dorsch, W.A., Fan, B., Cochran, J.E., Halas, S., Harrington, E.M., Hogan, J.K., Howe, D., Huang, H., Jacobs, D.H., Laitinen, L.M., Liao, S., Mahajan, S., Marone, V., Martinez-Botella, G., McCarthy, P., Messersmith, D., Namchuk, M., Oh, L., Penney, M.S., Pierce, A.C., Raybuck, S.A., Rugg, A., Salituro, F.G., Saxena, K., Shannon, D., Shlyakter, D., Swenson, L., Tian, S.K., Town, C., Wang, J., Wang, T., Wannamaker, M.W., Winquist, R.J. and Zuccola, H.J., 2015. Discovery of VX-509 (Decernotinib): A potent and selective Janus Kinase 3 inhibitor for the treatment of autoimmune diseases. *J. med. Chem.,* **58**: 7195-7216. https://doi.org/10.1021/acs.jmedchem.5b00301

Fleischmann, R., Kremer, J., Cush, J., Schulze-Koops, H., Connell, C.A., Bradley, J.D., Gruben, D., Wallenstein, G.V., Zwillich, S.H., Kanik, K.S. and Investigators, O.S., 2012. Placebo-controlled trial of tofacitinib monotherapy in rheumatoid arthritis. *N. Engl. J. Med.,* **367**: 495-507. https://doi.org/10.1056/NEJMoa1109071

Goedken, E.R., Argiriadi, M.A., Banach, D.L., Fiamengo, B.A., Foley, S.E., Frank, K.E., George, J.S., Harris, C.M., Hobson, A.D., Ihle, D.C., Marcotte, D., Merta, P.J., Michalak, M.E., Murdock, S.E., Tomlinson, M.J. and Voss, J.W., 2015. Tricyclic covalent inhibitors selectively target Jak3 through an active site thiol. *J. biol. Chem.,* **290**: 4573-4589. https://doi.org/10.1074/jbc.M114.595181

Guillon, J., Le Borgne, M., Rimbault, C., Moreau, S., Savrimoutou, S., Pinaud, N., Baratin, S., Marchivie, M., Roche, S., Bollacke, A., Pecci, A., Alvarez, L., Desplat, V. and Jose, J., 2013. Synthesis and biological evaluation of novel substituted pyrrolo[1,2-a]quinoxaline derivatives as inhibitors of the human protein kinase CK2. *Eur. J. med. Chem.,* **65**: 205-222. https://doi.org/10.1016/j.ejmech.2013.04.051

Hanwell, M.D., Curtis, D.E., Lonie, D.C., Vandermeersch, T., Zurek, E. and Hutchison, G.R., 2012. Avogadro: an advanced semantic chemical editor, visualization, and analysis platform. *J. Cheminform.,* **4**: 17. https://doi.org/10.1186/1758-2946-4-17

Haselmayer, P., Camps, M., Liu-Bujalski, L., Nguyen, N., Morandi, F., Head, J., O'Mahony, A., Zimmerli, S. C., Bruns, L., Bender, A.T., Schroeder, P. and Grenningloh, R., 2019. Efficacy and pharmacodynamic modeling of the BTK inhibitor evobrutinib in autoimmune disease models. *J. Immunol.,* **202**: 2888-2906. https://doi.org/10.4049/jimmunol.1800583

Hennessy, E.J., Chuaqui, C., Ashton, S., Colclough, N., Cross, D.A., Debreczeni, J.E., Eberlein, C., Gingipalli, L., Klinowska, T.C., Orme, J.P., Sha, L. and Wu, X., 2016. Utilization of structure-based design to identify novel, irreversible inhibitors of EGFR harboring the T790M mutation. *ACS med. Chem. Lett.,* **7**: 514-519. https://doi.org/10.1021/acsmedchemlett.6b00058

Jaime-Figueroa, S., De Vicente, J., Hermann, J., Jahangir, A., Jin, S., Kuglstatter, A., Lynch, S.M., Menke, J., Niu, L., Patel, V., Shao, A., Soth, M., Vu, M.D. and Yee, C., 2013. Discovery of a series of novel 5H-pyrrolo[2,3-b]pyrazine-2-phenyl ethers, as potent JAK3 kinase inhibitors. *Bioorg. med. Chem. Lett.,* **23**: 2522-2526. https://doi.

org/10.1016/j.bmcl.2013.03.015

Kempson, J., Ovalle, D., Guo, J., Wrobleski, S.T., Lin, S., Spergel, S.H., Duan, J.J., Jiang, B., Lu, Z., Das, J., Yang, B.V., Hynes, J., Jr., Wu, H., Tokarski, J., Sack, J.S., Khan, J., Schieven, G., Blatt, Y., Chaudhry, C., Salter-Cid, L.M., Fura, A., Barrish, J.C., Carter, P.H. and Pitts, W.J., 2017. Discovery of highly potent, selective, covalent inhibitors of JAK3. *Bioorg. med. Chem. Lett.,* **27**: 4622-4625. https://doi.org/10.1016/j.bmcl.2017.09.023

Kotyla, P.J., 2018. Are Janus kinase inhibitors superior over classic biologic agents in RA patients? *Biomed. Res. Int.,* **2018**: 7492904. https://doi.org/10.1155/2018/7492904

Lynch, S.M., DeVicente, J., Hermann, J.C., Jaime-Figueroa, S., Jin, S., Kuglstatter, A., Li, H., Lovey, A., Menke, J., Niu, L., Patel, V., Roy, D., Soth, M., Steiner, S., Tivitmahaisoon, P., Vu, M.D., and Yee, C., 2013. Strategic use of conformational bias and structure based design to identify potent JAK3 inhibitors with improved selectivity against the JAK family and the kinome. *Bioorg. med. Chem. Lett.,* **23**: 2793-2800. https://doi.org/10.1016/j.bmcl.2013.02.012

Markham, A., 2017. Baricitinib: First global approval. *Drugs,* **77**: 697-704. https://doi.org/10.1007/s40265-017-0723-3

Martel-Pelletier, J., Lajeunesse, D., Reboul, P. and Pelletier, J.P., 2003. Therapeutic role of dual inhibitors of 5-LOX and COX, selective and non-selective non-steroidal anti-inflammatory drugs. *Annls Rheum. Dis.,* **62**: 501-509. https://doi.org/10.1136/ard.62.6.501

Meier, F.M. and McInnes, I.B., 2014. Small-molecule therapeutics in rheumatoid arthritis: scientific rationale, efficacy and safety. *Best Pract. Res. clin. Rheumatol.,* **28**: 605-624. https://doi.org/10.1016/j.berh.2014.10.017

Morris, G.M., Huey, R., Lindstrom, W., Sanner, M.F., Belew, R.K., Goodsell, D.S. and Olson, A.J., 2009. AutoDock4 and AutoDockTools4: Automated docking with selective receptor flexibility. *J. Comput. Chem.,* **30**: 2785-2791. https://doi.org/10.1002/jcc.21256

Onuora, S., 2014. Rheumatoid arthritis: can tofacitinib be used as first-line monotherapy for RA? *Nat. Rev. Rheumatol.,* **10**: 443-443. https://doi.org/10.1038/nrrheum.2014.108

Orme, M.E., Macgilchrist, K.S., Mitchell, S., Spurden, D. and Bird, A., 2012. Systematic review and network meta-analysis of combination and monotherapy treatments in disease-modifying antirheumatic drug-experienced patients with rheumatoid arthritis: analysis of American College of Rheumatology criteria scores 20, 50, and 70. *Biologics,* **6**: 429-464. https://doi.org/10.2147/BTT.S36707

Park, J.K., Byun, J.Y., Park, J.A., Kim, Y.Y., Lee, Y.J., Oh, J.I., Jang, S.Y., Kim, Y.H., Song, Y.W., Son, J., Suh, K.H., Lee, Y.M. and Lee, E.B., 2016. HM71224, a novel Bruton's tyrosine kinase inhibitor, suppresses B cell and monocyte activation and ameliorates arthritis in a mouse model: a potential drug for rheumatoid arthritis. *Arthritis Res. Ther.,* **18**: 91. https://doi.org/10.1186/s13075-016-0988-z

Patinote, C., Bou Karroum, N., Moarbess, G., Deleuze-Masquefa, C., Hadj-Kaddour, K., Cuq, P., Diab-Assaf, M., Kassab, I. and Bonnet, P.A., 2017. Imidazo[1,2-a]pyrazine, Imidazo[1,5-a]quinoxaline and Pyrazolo[1,5-a]quinoxaline derivatives as IKK1 and IKK2 inhibitors. *Eur. J. med. Chem.,* **138**: 909-919. https://doi.org/10.1016/j.ejmech.2017.07.021

Pereira, J.A., Pessoa, A.M., Cordeiro, M.N., Fernandes, R., Prudencio, C., Noronha, J.P. and Vieira, M., 2015. Quinoxaline, its derivatives and applications: A state of art review. *Eur. J. med. Chem.,* **97**: 664-672. https://doi.org/10.1016/j.ejmech.2014.06.058

Qin, X., Han, X., Hu, L., Li, Z., Geng, Z., Wang, Z., Zeng, C. and Xiao, X., 2015. Design, synthesis and biological evaluation of quinoxalin-2(1H)-one derivatives as EGFR tyrosine kinase inhibitors. *Anticancer Agents med. Chem.,* **15**: 267-273. https://doi.org/10.2174/1871520615021501161733 57

Rice, P., Longden, I. and Bleasby, A., 2000. EMBOSS: the European Molecular Biology Open Software Suite. *Trends Genet.,* **16**: 276-277. https://doi.org/10.1016/S0168-9525(00)02024-2

Roskoski, R., Jr., 2016. Janus kinase (JAK) inhibitors in the treatment of inflammatory and neoplastic diseases. *Pharmacol. Res.,* **111**: 784-803. https://doi.org/10.1016/j.phrs.2016.07.038

Russell, S.M., Johnston, J.A., Noguchi, M., Kawamura, M., Bacon, C.M., Friedmann, M., Berg, M., McVicar, D.W., Witthuhn, B.A., Silvennoinen, O., Goldman, A.S., Schmalstieg, F.C., Ihie, J.N., O'Shea, J.J. and Leonard, W.J., 1994. Interaction of IL-2R beta and gamma c chains with Jak1 and Jak3: implications for XSCID and XCID. *Science,* **266**: 1042-1045. https://doi.org/10.1126/science.7973658

Russell, S.M., Tayebi, N., Nakajima, H., Riedy, M.C., Roberts, J.L., Aman, M.J., Migone, T.S., Noguchi,

M., Markert, M.L., Buckley, R.H., O'Shea, J.J. and Leonard, W.J., 1995. Mutation of Jak3 in a patient with SCID: essential role of Jak3 in lymphoid development. *Science,* **270**: 797-800. https://doi.org/10.1126/science.270.5237.797

Schwartz, D.M., Kanno, Y., Villarino, A., Ward, M., Gadina, M. and O'Shea, J.J., 2017. JAK inhibition as a therapeutic strategy for immune and inflammatory diseases. *Nat. Rev. Drug. Discov.,* **17**: 78. https://doi.org/10.1038/nrd.2017.267

Singh, J.A., Christensen, R., Wells, G.A., Suarez-Almazor, M.E., Buchbinder, R., Lopez-Olivo, M.A., Tanjong Ghogomu, E. and Tugwell, P., 2009. Biologics for rheumatoid arthritis: an overview of Cochrane reviews. *Cochrane Database Syst. Rev.*, **4**: CD007848. https://doi.org/10.1002/14651858.CD007848

Smolen, J.S., Landewe, R., Bijlsma, J., Burmester, G., Chatzidionysiou, K., Dougados, M., Nam, J., Ramiro, S., Voshaar, M., van Vollenhoven, R., Aletaha, D., Aringer, M., Boers, M., Buckley, C.D., Buttgereit, F., Bykerk, V., Cardiel, M., Combe, B., Cutolo, M., van Eijk-Hustings, Y., Emery, P., Finckh, A., Gabay, C., Gomez-Reino, J., Gossec, L., Gottenberg, J.E., Hazes, J.M.W., Huizinga, T., Jani, M., Karateev, D., Kouloumas, M., Kvien, T., Li, Z., Mariette, X., McInnes, I., Mysler, E., Nash, P., Pavelka, K., Poor, G., Richez, C., van Riel, P., Rubbert-Roth, A., Saag, K., da Silva, J., Stamm, T., Takeuchi, T., Westhovens, R., de Wit, M. and van der Heijde, D., 2017. EULAR recommendations for the management of rheumatoid arthritis with synthetic and biological disease-modifying antirheumatic drugs: 2016 update. *Annls Rheum. Dis.,* **76**: 960-977. https://doi.org/10.1136/annrheumdis-2016-210715

Soth, M., Hermann, J.C., Yee, C., Alam, M., Barnett, J.W., Berry, P., Browner, M.F., Frank, K., Frauchiger, S., Harris, S., He, Y., Hekmat-Nejad, M., Hendricks, T., Henningsen, R., Hilgenkamp, R., Ho, H., Hoffman, A., Hsu, P.Y., Hu, D.Q., Itano, A., Jaime-Figueroa, S., Jahangir, A., Jin, S., Kuglstatter, A., Kutach, A.K., Liao, C., Lynch, S., Menke, J., Niu, L., Patel, V., Railkar, A., Roy, D., Shao, A., Shaw, D., Steiner, S., Sun, Y., Tan, S.L., Wang, S. and Vu, M.D., 2013. 3-Amido pyrrolopyrazine JAK kinase inhibitors: development of a JAK3 vs JAK1 selective inhibitor and evaluation in cellular and in vivo models. *J. med. Chem.,* **56**: 345-356. https://doi.org/10.1021/jm301646k

Sterling, J., Herzig, Y., Goren, T., Finkelstein, N., Lerner, D., Goldenberg, W., Miskolczi, I., Molnar, S., Rantal, F., Tamas, T., Toth, G., Zagyva, A., Zekany, A., Finberg, J., Lavian, G., Gross, A., Friedman, R., Razin, M., Huang, W., Krais, B., Chorev, M., Youdim, M.B. and Weinstock, M., 2002. Novel dual inhibitors of AChE and MAO derived from hydroxy aminoindan and phenethylamine as potential treatment for Alzheimer's disease. *J. med. Chem.,* **45**: 5260-5279. https://doi.org/10.1021/jm020120c

Tanaka, Y., Hirata, S., Saleem, B. and Emery, P., 2013. Discontinuation of biologics in patients with rheumatoid arthritis. *Clin. exp. Rheumatol.,* **31**(4 Suppl 78): S22-27.

Tariq, S., Alam, O. and Amir, M., 2018a. Synthesis, anti-inflammatory, p38alpha MAP kinase inhibitory activities and molecular docking studies of quinoxaline derivatives containing triazole moiety. *Bioorg. Chem.,* **76**: 343-358. https://doi.org/10.1016/j.bioorg.2017.12.003

Tariq, S., Somakala, K. and Amir, M., 2018b. Quinoxaline: An insight into the recent pharmacological advances. *Eur. J. med. Chem.,* **143**: 542-557. https://doi.org/10.1016/j.ejmech.2017.11.064

Taylor, P.C., 2019. Clinical efficacy of launched JAK inhibitors in rheumatoid arthritis. *Rheumatology, (Oxford),* **58**(Supplement_1): 17-26. https://doi.org/10.1093/rheumatology/key225

Thoma, G., Nuninger, F., Falchetto, R., Hermes, E., Tavares, G.A., Vangrevelinghe, E. and Zerwes, H.G., 2011. Identification of a potent Janus kinase 3 inhibitor with high selectivity within the Janus kinase family. *J. Med. Chem.,* **54**: 284-288. https://doi.org/10.1021/jm101157q

Trott, O. and Olson, A.J., 2010. AutoDock Vina: improving the speed and accuracy of docking with a new scoring function, efficient optimization, and multithreading. *J. comput. Chem.,* **31**: 455-461 .https://doi.org/10.1002/jcc.21334

Walker, J.G., Ahern, M.J., Coleman, M., Weedon, H., Papangelis, V., Beroukas, D., Roberts-Thomson, P.J., and Smith, M.D., 2006a. Changes in synovial tissue Jak-STAT expression in rheumatoid arthritis in response to successful DMARD treatment. *Annls Rheum. Dis.,* **65**: 1558-1564. https://doi.org/10.1136/ard.2005.050385

Walker, J.G., Ahern, M.J., Coleman, M., Weedon, H., Papangelis, V., Beroukas, D., Roberts-Thomson, P.J. and Smith, M.D., 2006b. Expression of Jak3, STAT1, STAT4, and STAT6 in inflammatory arthritis: unique Jak3 and STAT4 expression in dendritic cells in seropositive rheumatoid arthritis.

Annls Rheum. Dis., **65**: 149-156. https://doi.org/10.1136/ard.2005.037929

Wu, H., Huang, Q., Qi, Z., Chen, Y., Wang, A., Chen, C., Liang, Q., Wang, J., Chen, W., Dong, J., Yu, K., Hu, C., Wang, W., Liu, X., Deng, Y., Wang, L., Wang, B., Li, X., Gray, N. and Liu, Q., 2017. Irreversible inhibition of BTK kinase by a novel highly selective inhibitor CHMFL-BTK-11 suppresses inflammatory response in rheumatoid arthritis model. *Scient. Rep.,* **7**: 466. https://doi.org/10.1038/s41598-017-00482-4

Wu, P., Su, Y., Guan, X., Liu, X., Zhang, J., Dong, X., Huang, W. and Hu, Y., 2012. Identification of novel piperazinylquinoxaline derivatives as potent phosphoinositide 3-kinase (PI3K) inhibitors. *PLoS One,* **7**: e43171. https://doi.org/10.1371/journal.pone.0043171

Pakistan J. Zool., pp 1-13, 2021. **DOI**: https://dx.doi.org/10.17582/journal.pjz/20191010081058

Supplementary Material

Dual Targeting of Janus Kinase and Bruton's Tyrosine Kinase: A New Approach to Control the Pathogenesis of Rheumatoid Arthritis

Neelam Pery[1]*, Fatima Ijaz[1], Nayab Batool Rizvi[1], Munawar Ali Munawar[1] and Muhammad Imtiaz Shafiq[2]*

[1]*Institute of Chemistry, University of the Punjab, Lahore, Pakistan 54590*
[2]*Institute of Biochemistry and Biotechnology, University of the Punjab, Lahore-54590*

SEQUENCE ALIGNMENT OF JAK3 AND BTK

The pair wise alignment tool EMBOSS Matcher was used to align the sequences. The results obtained show 32.7% identity (67/205), 58.5% similarity (120/205) and 4.9% (10/205) gaps with a score of 266. The basic purpose of this sequence alignment was to identify the regions that have same or equivalent residues and offer similar interactions.

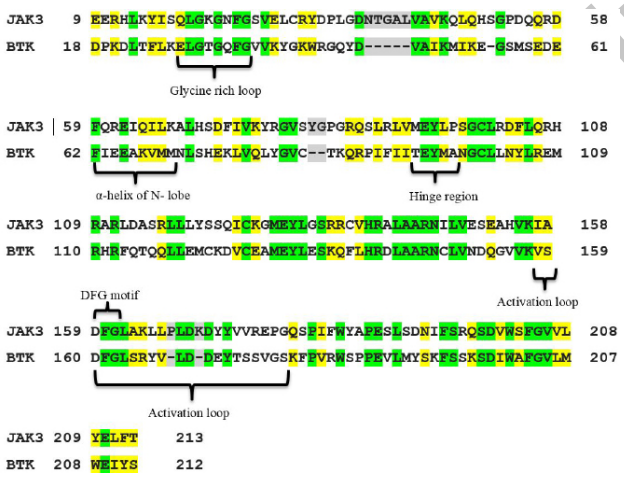

(Pairwise sequence alignment of JAK3 and BTK. Green represents same residues, yellow are equivalent while grey represent the gaps.)

SYNTHESIS PROCEDURE

An equimolar mixture of 4-nitro-o-phenylenediamine (0.025 mol, 3.83 g) and substituted vicinal diketone (0.025 mol) was refluxed in 40 mL of ethanol: acetic acid mixture (1:1) for 2-3 hours. Precipitates were formed on cooling the resulting mixture. The precipitates were filtered, washed with ethanol and dried to obtain pure product of substituted 6-nitroquinoxaline.

A mixture containing substituted 6-nitroquinoxaline (0.02 moles) and 10 % Pd/C in absolute ethanol (30-35 mL) was heated with continuous stirring.in a round bottom flask equipped with a dropping funnel and a reflux condenser flask. 6 mL of hydrazine monohydrate was added at the start of refluxing. The reaction mixture was refluxed for 2 hrs. The contents of the flask were filtered in hot state. Crystals of the corresponding aminoquinoxaline were obtained on cooling which were then filtered, washed with ethanol and dried.

Analytical data of synthesized compounds

Compound 1: 6-Nitroquinoxaline

Physical appearance: Shiny straw-colored crystals
Yield: 92%
Melting Point: 174-175 °C
FT-IR: υ (cm^{-1}): 3060 (Ar-H); 1615 (C=N); 1586, 1550, 1525 (Aromatic ring); 1490, 1346 (NO_2); 872 (C-NO_2)
^{1}H NMR: ($CDCl_3$, 500MHz): δ_H: 9.04-9.02 (3H, m, H-2, H-3, H-5), 8.57-8.55 (1H, dd, J = 9.15 Hz, 2.3 Hz, H-7), 8.29 (1H, d, J = 9.15 Hz, H-8)

Compound 2: Quinoxalin-6-amine

Physical appearance: Dirty green crystals
Yield:90 %
Melting Point: 160-162 °C
FT-IR: υ (cm^{-1}): 3388, 3310 (NH_2); 3160 (Ar-H); 1630 (C=N), 1606, 1502, 1460 (Aromatic ring); 1300 (C-N 'amine')
^{1}H NMR: ($CDCl_3$, 500MHz): δ_H: 8.66 (1H, d, J = 1.5 Hz, H-3), 8.55 (1H, d, J = 2.3 Hz, H-2), 7.88 (1H, d, J = 9.15 Hz, H-8), 7.18-7.20 (1H, dd, J = 9.2 Hz, J = 3.05 Hz, H-7), 7.14 (1H, d, J = 2.3 Hz, H-5), 4.23 (2H, s, NH_2)

* Corresponding author: neelam.wafa@gmail.com; imtiaz.ibb@pu.edu.pk
0030-9923/2021/0004-0001 $ 9.00/0

Compound 3: 2,3-dimethyl-6-nitroquinoxaline
Physical Appearance: Shiny golden pink precipitates
Yield: (94 %)
Melting Point: 129-130 °C
FT-IR: υ (cm^{-1}): 3044 (Ar-H); 1618 (C=N); 1579, 1493, 1451 (Aromatic ring); 1523, 1343 (NO_2); 848 (C-NO_2)
^{1}H NMR: ($CDCl_3$, 500MHz): δ_H: 8.95 (1H, s, H-5), 8.48 (1H, d, *J* = 8.4 Hz, H-7), 8.22 (1H, d, *J* = 9.15 Hz, H-8), 2.86 (3H, s, 3H-1'), 2.84 (3H, s, 3H-1'')

Compound 4: 2,3-dimethylquinoxalin-6-amine
Physical appearance: Yellow crystalline solid
Yield: 87 %
Melting Point: 187-188 °C
FT-IR: υ (cm^{-1}): 3326, 3333 (NH_2); 3020 (Ar-H); 1639 (C=N), 1621, 1563, 1503, 1468 (Aromatic ring); 1250 (C-N 'amine')
^{1}H NMR: ($CDCl_3$, 500MHz): δ_H: 8.09 (1H, d, *J* = 8.4 Hz, H-8), 7.76 (1H, d, *J* = 8.4 Hz, H-5), 7.08-7.10 (1H, m, H-7), 4.07 (2H, s, NH_2), 2.65-2.67 (6H, m, 3H-1', 3H-1'')

Compound 5: 2,3-di(furan-2-yl)-6-nitroquinoxaline
Physical appearance: Dark brown crystals
Yield: 96 %
Melting Point: 160-161 °C
FT-IR: υ (cm^{-1}): 3097 (Ar-H); 1618 (C=N); 1567, 1523, 1467 (Aromatic ring); 1482, 1339 (NO_2); 828 (C-NO_2)
^{1}H NMR: (DMSO, 500MHz): δ_H: 8.9 (1H, d, *J* = 2 Hz, H-5), 8.59-8.62 (1H, dd, *J* = 9.5 Hz, 2.5 Hz, H-7), 8.31 (1H, d, *J* = 9 Hz, H-8), 7.90-7.91 (2H, two closely merged doublets, H-5', H-5''), 7.03 (1H, d, *J* = 3.5 Hz, H-3'), 7.00 (1H, d, *J* = 3.5 Hz, H-3''), 6.80-6.81 (2H, m, H-4', H-4'')

Compound 6: 2,3-di(furan-2-yl)quinoxalin-6-amine
Physical appearance: Straw-colored crystals
Yield: 88 %
Melting Point: 192-194 °C
FT-IR: υ (cm^{-1}): 3459, 3305 (NH_2); 3199, 3118 (Ar-H); 1630 (C=N), 1596, 1574, 1529, 1486 (Aromatic ring); 1340 (C-N 'amine')
^{1}H NMR: ($CDCl_3$, 500MHz): δ_H: 7.92 (1H, d, *J* = 9.0 Hz, H-8), 7.6 (1H, s, H-5''), 7.58 (1H, d, *J* = 0.5 Hz, H-5'), 7.20 (1H, d, *J* = 2.5 Hz, H-3''), 7.15-7.17 (1H, dd, *J* = 9.0 Hz, *J* = 2.5 Hz, H-3'), 6.52-6.56 (4H, m, H-5, H-7, H-4', H-4''), 4.27 (2H, s, NH_2)

Compound 7: 2,3-diphenyl-6-nitroquinoxaline
Physical appearance: Shiny off-white precipitates
Yield: 95 %
Melting Point: 192-194 °C
FT-IR: υ (cm^{-1}): 3051 (Ar-H); 1616 (C=N); 1515, 1337 (NO_2); 837 (C-NO_2)
^{1}H NMR: ($CDCl_3$, 500MHz): δ_H: 9.08 (1H, d, *J* = 2.3 Hz, H-5), 8.55-8.53 (1H, dd, *J* = 9.15 Hz, 2.3 Hz, H-7), 8.3 (1H, d, *J* = 9.15, H-8), 7.59-7.55 (4H, m, H-3', H-5', H-3'', H-5''),7.43-7.36 (6H, m, H-2', H-4', H-6', H-2'', H-4'', H-6'')

Compound 8: 2,3-diphenylquinoxalin-6-amine
Physical appearance: Yellow crystals
Yield: 86 %
Melting Point: 180-181 °C
FT-IR: υ (cm^{-1}): 3445, 3317 (NH_2); 3212 (Ar-H); 1638 (C=N), 1613, 1490 (Aromatic ring); 1349 (C-N 'amine')
^{1}H NMR: ($CDCl_3$, 500MHz): δ_H: 8.00 (1H, d, *J* = 9.15 Hz, H-8), 7.52-7.59 (4H, m, H-3', H-5', H-3'', H-5''), 7.44-7.45 (2H, m, H-4', H-4''), 7.24-7.39 (8H, m, H-5, H-7, H-2', H-6', H-2'', H-6'', NH_2)

Compound 9: 7-Nitro-11H-indeno[1,2-b]quinoxalin-11-one (9a) / 8-Nitro-11H-indeno[1,2-b]quinoxalin-11-one (9b)
Physical appearance: Yellow orange precipitates
Yield: 91 %
Melting Point: 292-294 °C
FT-IR: υ (cm^{-1}): 3070 (Ar-H); 1721 (C=O); 1607, 1573, 1501 (Aromatic ring); 1536, 1350 (NO_2)
^{1}H NMR: ($CDCl_3$, 500MHz): δ_H: "9.12 (1H, d, *J* = 2.5Hz, H-8_a), 9.02 (1H, d, *J* = 2.5Hz, H-11_b), 8.59-8.61 (1H, dd, *J* = 9Hz, 2.5Hz, H-10_a), 8.51-8.53 (1H, dd, *J* = 9Hz, 2.5Hz, H-9_b), 8.41 (1H, d, *J* = 9Hz, H-8_b), 8.28 (1H, d, *J* = 9Hz, H-11_a), 8.19-8.21 (2H, dd, *J* = 7.5Hz, 0.5Hz, H-5_a, H-5_b), 8.01 (2H, d, *J* = 7.5Hz, H-2_a, H-2_b), 7.85-7.88 (2H, dt, *J* = 7.5Hz, 1Hz, H-3_a, H-3_b), 7.71-7.74 (2H, dt, *J* = 7.5Hz, 1Hz, H-4_a, H-4_b)"

Compound 10: 8-Amino-11H-indeno[1,2-b]quinoxalin-11-one (10a) / 7-Amino-11H-indeno[1,2-b]quinoxalin-11-one (10b)
Physical appearance: Orange precipitates
Yield: 85 %
Melting Point: 238-240 °C
FT-IR: υ (cm^{-1}): 3322, 3300 (NH_2); 3160 (Ar-H); 1630 (C=N), 1587, 1578, 1479 (Aromatic ring); 1342 (C-N 'amine')
^{1}H NMR: ($CDCl_3$, 500MHz): δ_H: "8.18 (1H, d, *J* = 6Hz, H-5_b), 8.07 (1H, d, *J* = 7.5Hz, H-5_a), 7.94-7.97 (2H, m, H-2_a, H-2_b), 7.81 (1H, d, *J* = 7.5Hz, H-3_a), 7.63 (1H, d, *J* = 6Hz, H-3_b), 7.42-7.50 (4H, m, H-4_a, H-4_b, H-8_b,H-11_a), 7.16-7.19 (2H, m, H-8_a, H-10_a), 7.13 (1H, d, *J* = 8.5Hz, H-9_b), 6.88 (1H, s, H-11_b), 4.17 (2H, s, $NH_{2\ a}$), 4.09 (2H, s, $NH_{2\ b}$)"